Extreme Statistics and Spacing Distribution in a Brownian Gas Correlated by Resetting

Marco Biroli[1], Hernan Larralde[2], Satya N. Majumdar[1], and Grégory Schehr[3]

[1]*LPTMS, CNRS, Univ. Paris-Sud, Université Paris-Saclay, 91405 Orsay, France*
[2]*Instituto de Ciencias Fisicas, UNAM, Avenida Universidad s/n, CP 62210 Cuernavaca, Morelos, Mexico*
[3]*Sorbonne Université, Laboratoire de Physique Théorique et Hautes Energies,*
CNRS UMR 7589, 4 Place Jussieu, 75252 Paris Cedex 05, France

We study a one-dimensional gas of N Brownian particles that diffuse independently, but are simultaneously reset to the origin at a constant rate r. The system approaches a nonequilibrium stationary state with long-range interactions induced by the simultaneous resetting. Despite the presence of strong correlations, we show that several observables can be computed exactly, which include the global average density, the distribution of the position of the kth rightmost particle, and the spacing distribution between two successive particles. Our analytical results are confirmed by numerical simulations. We also discuss a possible experimental realization of this resetting gas using optical traps.

While the properties of a gas of noninteracting particles are well understood, those of an interacting gas, in particular in the presence of a long-range interaction between particles, are much less so. A notable exception is the celebrated Dyson log gas in one dimension, that appears in the spectral statistics of random matrix theory. Indeed, the statistics of the eigenvalues of Gaussian random matrices play a major role in several areas of science, from nuclear physics, quantum chaos, and mesoscopic transport, all the way to finance and information theory [1–4]. For an $N \times N$ matrix (real symmetric, complex Hermitian, or quaternionic symplectic) with independent Gaussian entries, the joint probability distribution function (JPDF) of the N real eigenvalues $\{x_i\}$ can be expressed as a Boltzmann weight $P[\{x_i\}] \propto \exp(-\beta E[\{x_i\}])$ with the energy given by $E[\{x_i\}] = \frac{1}{2}\sum_{i=1}^{N} x_i^2 - \frac{1}{2}\sum_{i \neq j} \ln |x_i - x_j|$, where the Dyson index $\beta = 1, 2, 4$ corresponds to the three symmetry classes mentioned above [1,2]. Thus, the eigenvalues x_i can be interpreted as the positions of N particles on a line in the presence of a confining harmonic potential, with pairwise logarithmic repulsion between them. This is Dyson's log gas [5], which has been a fundamental cornerstone [2] in understanding the role of strong correlations on several spectral observables such as the average density of eigenvalues [6], the largest eigenvalue [7–10] (i.e., the position of the rightmost particle in the gas), and the spacing distribution between successive eigenvalues [1,2,11]. These observables can be computed exactly for the log gas, thanks to a special analytical structure of the particular form of the JPDF [1,2]. Moreover, they have been measured experimentally in a variety of systems, from nuclear physics and quantum chaos [12] to liquid crystals [13] and fiber lasers [14]. Unfortunately, there exist very few long-ranged correlated gases, even in one dimension,

for which these observables can be computed, with perhaps the exception of the 1D jellium model where the pairwise repulsion is linear [15–21].

It is therefore natural to look for other experimentally realizable long-ranged correlated particle systems for which these observables can be computed analytically. Motivated by the recent theoretical and experimental advances in the field of stochastic resetting [22–25], in this Letter, we propose a new many-particle model that, despite the presence of strong correlations induced by dynamics, is solvable for all the spectral observables mentioned above.

A single particle subjected to stochastic resetting has been studied extensively over the past decade [26–42]. Consider, for simplicity, a single Brownian particle diffusing on a line with diffusion constant D, starting at the origin. With rate r, the particle's position is reset back to the origin and the free diffusion restarts. This resetting move breaks detailed balance and drives the system into a nonequilibrium stationary state where the position distribution becomes non-Gaussian [26,27]:

$$P_{\text{stat}}(x) = \frac{1}{2}\sqrt{\frac{r}{D}}\exp\left(-|x|\sqrt{r/D}\right). \quad (1)$$

This simple analytical prediction has been verified in recent experiments using holographic optical tweezers [39]. In this Letter, we consider N independent Brownian particles on a line, all starting at the origin, that are *simultaneously* reset to the origin with rate r (this is different from independently reset Brownian particles studied before [26,43]). This simultaneous resetting makes the system strongly correlated, and this correlation persists even in the resulting many-body nonequilibrium stationary state at long times. To see this, let us first compute the joint
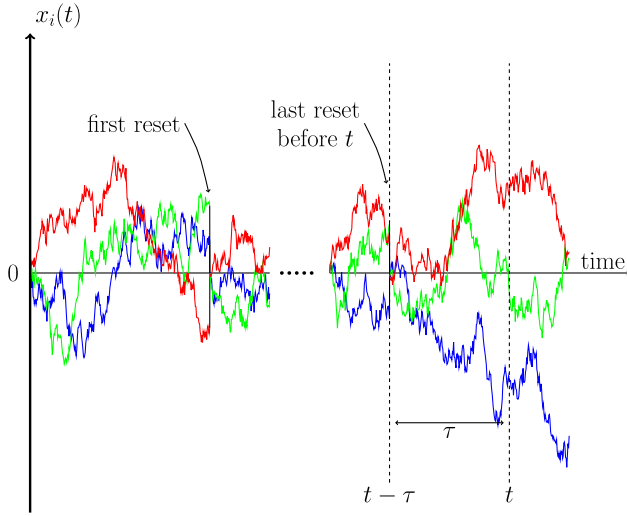
FIG. 1. Schematic trajectories of $N = 3$ Brownian motions undergoing simultaneous resetting to the origin at random times. The observation time is marked by t and the time of the last reset before t is marked by $t - \tau$. During the last period τ, the particles evolve independently as free Brownian motions.

distribution $P_r[\{x_i\}, t]$ of the positions x_i of the particles at time t (all starting at the origin), where the subscript r denotes the resetting with constant rate r. For $r = 0$, the particles evolve as N independent Brownian motions and their joint distribution just becomes a product of N independent Gaussians, given by

$$P_0[\{x_i\}, t] = \prod_{i=1}^{N} \frac{1}{\sqrt{4\pi Dt}} e^{-x_i^2/4Dt}. \quad (2)$$

To see how a nonzero r makes the particles correlated, we proceed as follows. We consider the interval $[0, t]$ and see how many resetting events occur in that interval. With a probability e^{-rt} there will be no resetting in $[0, t]$—in that case, the joint distribution at time t will be simply $P_0[\{x_i\}, t]e^{-rt}$. When there is at least one resetting event in $[0, t]$, we remark that the state of the system at time t depends only on the time elapsed since the last resetting before t. This is because every resetting event brings back all the particles to the origin and, hence, we only need to keep track of the time since the last resetting. This idea is illustrated in Fig. 1 where t is the observation time and $t - \tau$ is the time at which the last resetting occurs before t. Since the evolution between $t - \tau$ and t is free (i.e., without resetting), clearly the joint distribution of the positions at time t is simply $P_0[\{x_i\}, \tau]$. However, τ itself is a random variable, with a probability density $re^{-r\tau}$, and τ can vary from 0 to t. Hence we need to multiply $P_0[\{x_i\}, \tau]$ by $re^{-r\tau}d\tau$ and integrate τ from 0 to t. Adding these two contributions, i.e., no-resetting event and the multiple resettings, we get the joint distribution at time t as

$$P_r[\{x_i\}, t] = e^{-rt}P_0[\{x_i\}, t] + r\int_0^t d\tau e^{-r\tau}P_0[\{x_i\}, \tau]. \quad (3)$$

In the longtime limit, the first term in Eq. (3) drops out and we obtain the exact JPDF in the stationary state:

$$P_{\text{stat}}[\{x_i\}] = r\int_0^\infty d\tau e^{-r\tau} \prod_{i=1}^{N} \frac{1}{\sqrt{4\pi D\tau}} e^{-x_i^2/4D\tau}. \quad (4)$$

This is one of our main results, which merits a few remarks. We note that the joint distribution in the stationary state does not factorize (even though the integrand inside the integral has a factorized form), indicating that the particles are correlated in the steady state. The physical origin of these correlations can be traced back to the fact that, via simultaneous resetting, the particles are pushed together toward the origin, which creates an effective attraction between the particles. Note that these correlations or the effective interactions between particles in the steady state have a purely *dynamical* origin and are not inherent interactions between particles as in Dyson's log gas or in the 1D jellium model. The integral in Eq. (4) can, in fact, be performed explicitly,

$$P_{\text{stat}}[\{x_i\}] = \left(\frac{r}{2\pi D}\right)^{N/2} R_N^{(2-N)/2} K_{N/2-1}(R_N), \quad (5)$$

where $R_N = \sqrt{(r/D)}\sqrt{x_1^2 + \cdots + x_N^2}$ and $K_\nu(z)$ is the modified Bessel function of index ν. This makes the correlated nature of the gas manifest, since the JPDF does not factorize, though unlike the log gas the correlation is not pairwise but rather "all to all." Finally, to see that this resetting gas indeed has long-range correlations, we compute the two-point correlations from the JPDF in Eq. (4). Noting that $\langle x_i x_j \rangle - \langle x_i \rangle \langle x_j \rangle = 0$ (for $i \neq j$) trivially, the first nontrivial correlator is given by

$$\langle x_i^2 x_j^2 \rangle - \langle x_i^2 \rangle \langle x_j^2 \rangle = \frac{4D^2}{r^2}, \quad \forall \; i, j, \quad (6)$$

which manifestly demonstrates the long-range correlations.

Given the JPDF in Eq. (4), our goal, motivated by the studies in the Dyson log gas, is to compute three natural observables, namely, (i) the average density, (ii) extreme statistics, and (iii) the spacing distribution between consecutive particles. The reason why these observables can be computed exactly can be seen in the structure of the JPDF in Eq. (4), where the integrand (modulo $e^{-r\tau}$) just corresponds to a set of N independent and Gaussian distributed random variables, parametrized by τ. For a fixed τ, we first compute the statistics of these observables for N independent and identically distributed Gaussian random variables and then integrate over τ. We will see that this simple mechanism leads to rather rich and interesting behaviors of these observables.

We start with the first basic observable, namely, the average density of particles in the stationary state, defined by $\rho(x, N) = (1/N)\langle \sum_{i=1}^N \delta(x - x_i) \rangle$, where $\langle \cdots \rangle$ denotes the average over the stationary measure in Eq. (4). The density $\rho(x, N)$ is normalized to unity and measures the
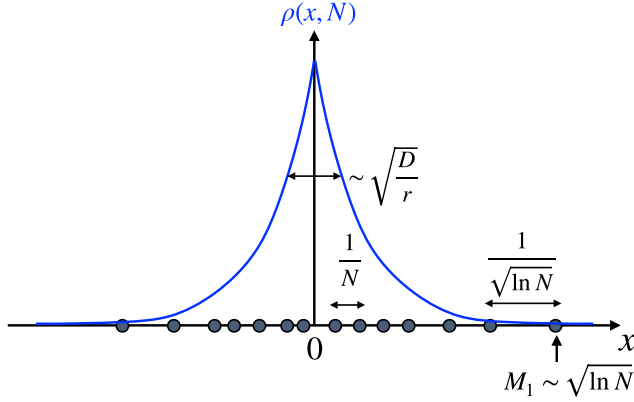
FIG. 2. The solid blue line shows the average density $\rho(x, N) = \sqrt{(r/4D)}e^{-\sqrt{r/D}|x|}$. The positions of the particles in a typical sample are shown schematically on the line with most particles living over a distance $\sqrt{D/r}$ around the origin. The typical spacing in the bulk $\sim 1/N$, while it is of order $\sim 1/\sqrt{\ln N}$ near the extreme edges of the sample. The typical position of the rightmost particle $M_1 \sim \sqrt{\ln N}$ for large N.

average fraction of particles in $[x, x + dx]$. Using the invariance of the JPDF in Eq. (4) under exchange of i and j, one sees that $\rho(x, N)$ is also the one-point function $\rho(x, N) = \int_{-\infty}^{\infty} dx_2 \cdots dx_N P_{\text{stat}}(x, x_2, \ldots, x_N)$. Then, given the factorization property in Eq. (4), we find that $\rho(x, N)$ coincides with the position distribution $P_{\text{stat}}(x)$ of a single particle given in Eq. (1) and plotted in Fig. 2. However, this does not mean that the particles are uncorrelated, as seen from the fact the JPDF in Eq. (4) does not factorize. Thus, $\rho(x, N)$ is independent of N and is supported over the full line. This is in contrast with other models with long-range pairwise repulsion, such as the Dyson log gas and the 1D jellium model, where the average density is supported over a finite interval. In the former case, it is the celebrated Wigner semicircular law [6] while, for the jellium, the average density is flat over a finite interval [15–18].

Moreover, from Eq. (1), one sees that the density decreases exponentially over a length scale $\sqrt{D/r}$ where most particles are concentrated in a typical sample (see Fig. 2). Hence, the typical spacing between particles in the bulk scales as $\sim O(1/N)$ for large N. While the average density extends over the full space, in a typical sample, the rightmost (or leftmost) particle is located at a distance of order $O(\sqrt{\ln N})$ from the center (see later). In addition, the spacing between two particles near these extremes scales as $1/\sqrt{\ln N} \gg 1/N$. Thus in a typical sample the gas is denser near the center and sparser near the extremes, as illustrated in Fig. 2.

Having computed the global density, we now probe the gas at a local level by studying the statistics of the positions of individual particles and the spacing between them. For this, it is convenient to first order the positions $\{x_1, x_2, \ldots, x_N\}$ and label them as $\{M_1 > M_2 > \cdots > M_N\}$,

where M_k denotes the position of the kth particle counted from the right. Thus $M_1 = \max\{x_1, x_2, \ldots, x_N\}$ denotes the global maximum, i.e., the position of the rightmost particle. This observable M_1 is well studied when the underlying random variables x_i are uncorrelated and its distribution is known to belong to the three famous universality classes, namely, Gumbel, Fréchet, and Weibull depending on the tails of the distribution of x_i [44–47]. There has been a lot of interest in computing the distribution of M_1 in the case where the random variables x_i are strongly correlated, and very few results are known in that case [47]. One well-known example corresponds to the Dyson log gas, where M_1 represents the largest eigenvalue of a Gaussian random matrix. In this case, the distribution of M_1, appropriately centered and scaled, follows the celebrated Tracy-Widom distribution [7–10]. Another solvable example corresponds to the 1D jellium model where the distribution is known to be different from the Tracy-Widom law [18,19]. Similarly, the statistics of the kth maximum have been studied for Dyson's log gas [7,8]. One of the main results of this Letter is to compute exactly the distribution of M_k for all k in the correlated resetting gas. Notably, for $k = 1$, we find a new extreme value distribution, which is different from the ones mentioned above.

We start by computing the PDF of M_k, i.e., the kth maximum of the ordered positions x_i that are distributed via the JPDF $P_{\text{stat}}[\{x_i\}]$ in Eq. (4). As for the JPDF, it is convenient to exploit the renewal structure in Eq. (3), also depicted graphically in Fig. 1. It is clear, then, that in the stationary state ($t \to \infty$ limit), the PDF of M_k can be expressed as

$$\text{Prob}(M_k = w) = r \int_0^{\infty} d\tau e^{-r\tau} \text{Prob}[M_k(\tau) = w], \quad (7)$$

where $M_k(\tau)$ is the kth maximum of a set of N independent Brownian motions each of duration τ, i.e., drawn from the Gaussian distribution $\exp[-x_i^2/(4D\tau)]/\sqrt{4\pi D\tau}$. The distribution of the kth maximum of N independent and identically distributed Gaussian random variables is well studied in the literature and is reproduced in the Supplemental Material [48]. Here we just state the main results. We set $k = \alpha N$ and take the limit of large N, keeping $0 < \alpha < 1$ fixed. In this limit, the distribution of $M_k(\tau)$ approaches a Gaussian form with mean $w^* = \sqrt{4D\tau} \, \text{erfc}^{-1}(2\alpha)$ and variance $\propto 1/N$ [here $\text{erfc}^{-1}(z)$ is the inverse of the complementary error function $\text{erfc}(z) = (2/\sqrt{\pi}) \int_z^{\infty} e^{-u^2} du$]. In the large N limit, the distribution of $M_k(\tau)$ essentially approaches a δ function centered at w^*, i.e., $\text{Prob}[M_k(\tau) = w] \to \delta[w - \sqrt{4D\tau} \, \text{erfc}^{-1}(2\alpha)]$. Substituting this behavior in Eq. (7), we arrive at

$$\text{Prob}(M_k = w) \approx \frac{1}{\Lambda(\alpha)} f\left(\frac{w}{\Lambda(\alpha)}\right), \qquad f(z) = 2ze^{-z^2}, \quad (8)$$
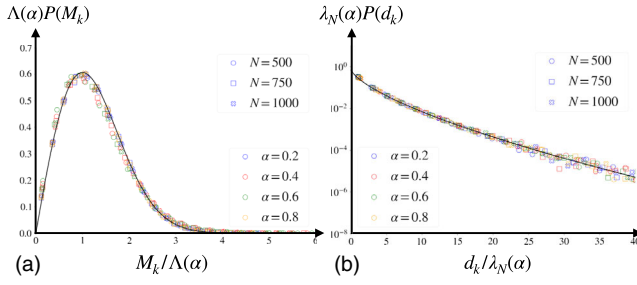
FIG. 3. (a) Scaled distribution of the position M_k of the kth particle from the right: $P(M_k) \approx \Lambda^{-1}(\alpha) f[M_k \Lambda^{-1}(\alpha)]$ with $\Lambda(\alpha)$ given below Eq. (8). The symbols represent the results of simulations, while the solid curve shows the scaling function $f(z)$ in Eq. (8). (b) Scaled distribution of the gap $d_k = M_k - M_{k+1}$ between the kth and the $(k+1)$th particle counted from the right: numerical simulations are in perfect agreement with the analytical scaling function $h(z)$ in Eq. (12). We used the parameter values $D = 0.5$ and $r = 1$.

with $z \geq 0$ and $\Lambda(\alpha) = \sqrt{4D/r}\,\mathrm{erfc}^{-1}(2\alpha)$. In the large N limit, the scaling function $f(z)$ is thus supported only over $z \geq 0$ and is universal; i.e., it is independent of α. For $\alpha = O(1)$, this gives us the behavior for the kth maximum in the bulk, while setting $\alpha = k/N$ with $k = O(1)$ we can probe the kth maximum near the global maximum M_1. In this limit, using $\mathrm{erfc}^{-1}(2k/N) \approx \sqrt{\ln N}$ to leading order for large N (independently of k), we see that $\Lambda(\alpha) \to L_N = \sqrt{4D \ln(N)/r}$. However, the distribution of M_k has exactly the same scaling function $f(z) = 2ze^{-z^2}\theta(z)$ as in Eq. (8) except that the scale factor $\Lambda(\alpha)$ gets replaced by L_N. These results are confirmed in our numerical simulations as shown in Fig. 3(a) for different values of α. Indeed the global maximum M_1, in particular, typically scales as $L_N \sim \sqrt{\ln N}$ for large N. Thus, even though, on average, the gas is spread over the full real line, in a typical sample, it is supported over an interval with length $L_N \sim \sqrt{\ln N}$.

The behavior of M_k in our correlated gas model is thus very different from the Dyson log gas or the 1D jellium model. In our model, the distributions of the kth maxima, both in and out of the bulk, are described by the same universal scaling function $f(z) = 2ze^{-z^2}\theta(z)$. This is in marked contrast to the Dyson log gas where the distributions of the maxima near the edge are similar to the Tracy-Widom distribution while, in the bulk, they are Gaussian [54]. Thus our result for $f(z)$ is a new extreme value distribution that was not encountered before.

We now turn to the distribution of the spacing (or gap) between two consecutive particles $d_k = M_k - M_{k+1}$. We can exploit again the renewal structure in Eq. (3) and write

$$\mathrm{Prob}(d_k = g) = r \int_0^\infty d\tau e^{-r\tau} \mathrm{Prob}[d_k(\tau) = g], \quad (9)$$

where $d_k(\tau) = M_k(\tau) - M_{k+1}(\tau)$ is the kth gap of N independent Brownian motions, each of duration τ. The

distribution of the gap $d_k(\tau)$ can be computed in the large N limit, by setting $k = \alpha N$ and using a saddle point method, detailed in Ref. [48]. We find that $d_k(\tau)$ has a simple exponential distribution,

$$\mathrm{Prob}[(d_k(\tau) = g] \approx \frac{bN}{\sqrt{\tau}} e^{-(bN/\sqrt{\tau})g}, \quad (10)$$

where $b = \exp\left\{-[\mathrm{erfc}^{-1}(2\alpha)]^2\right\}/\sqrt{4\pi D}$ is just a constant, independent of τ and N. Inserting this result in Eq. (9), and performing the change of variable $u = \sqrt{r\tau}$, we obtain

$$\mathrm{Prob}(d_k = g) \approx \frac{1}{\lambda_N(\alpha)} h\left(\frac{g}{\lambda_N(\alpha)}\right), \quad \lambda_N(\alpha) = \frac{1}{b\sqrt{rN}}, \quad (11)$$

where the normalized scaling function $h(z)$ is given by

$$h(z) = 2 \int_0^\infty du\, e^{-u^2 - z/u}. \quad (12)$$

The scaling function $h(z) \to \sqrt{\pi}$ as $z \to 0$ and has a stretched exponential tail $h(z) \sim e^{-3(z/2)^{2/3}}$ for large z (see Ref. [48]). Since $\alpha = k/N$, by choosing $k = 1, 2, 3, \ldots$, one can probe the first, second, third gap, etc. In this case $\alpha \sim O(1/N)$ is small for large N. We show in Ref. [48] that in this case, $\lambda_N(\alpha) \to \ell_N(k) = \sqrt{D/(rk^2 \ln N)}$. While the scale factor changes, the scaling function $h(z)$ is universal, i.e., independent of α. This universal result for $h(z)$ is verified in numerical simulations in Fig. 3(b). From Fig. 3(b) it is clear that $h(z)$ is a monotonically decreasing function of z with a maximum at $z = 0$. Thus two consecutive particles are most likely to be next to each other (with a zero gap), indicating an effective attraction between the particles. This is in stark contrast with the Dyson log gas case where, due to the pairwise repulsion between eigenvalues, the spacing distribution vanishes as the gap $g \to 0$: this is the celebrated Wigner surmise for the level repulsion in random matrix theory. In addition, in the Dyson log gas as well as in the 1D jellium model, the scaling functions of the spacing distribution are very different in the bulk and at the edges, again in sharp contrast with our result for the correlated resetting gas where the gap scaling function $h(z)$ in Eq. (12) is universal, i.e., independent of the index k of the gap.

To summarize, we have presented the exact solution of a resetting gas with long-range correlations in the steady state and computed several observables of interest. This includes the global average density, the distribution of the position of kth rightmost particle, and the spacing distribution between two consecutive particles. Our technique can be easily extended to compute other observables, e.g., the full counting statistics, i.e., the distribution of the number of particles in a given interval (this is presented in Ref. [48]). Our results can be generalized to higher dimensions in a straightforward way. Apart from the celebrated log gas, this

is one of the few solvable models with strong correlations. In addition, this resetting gas is also experimentally realizable. A single diffusing particle with resetting has been recently realized in optical trap experiments [40,41], where the particle is allowed to diffuse freely for a random time after which a trap is switched on. The particle is relaxed to its equilibrium in the trap using the "engineering swift equilibration" technique [55]. This mimics the resetting move of the particle to its equilibrium distribution. The same protocol, via the engineering swift equilibration technique, can possibly be implemented to simultaneously reset many noninteracting particles in the same optical trap. We thus hope that our analytical predictions will stimulate further experimental studies of such a resetting gas.

---

[1] M. L. Mehta, *Random Matrices* (Elsevier, New York, 2004).

[2] P. J. Forrester, *Log-Gases and Random Matrices* (London Mathematical Society Monographs, Princeton, 2010).

[3] G. Livan, M. Novaes, and P. Vivo, *Introduction to Random Matrices Theory and Practice*, Springer: SpringerBriefs in Mathematical Physics (2018), Vol. 26.

[4] M. Potters and J. P. Bouchaud, *A First Course in Random Matrix Theory: For Physicists, Engineers and Data Scientists* (Cambridge University Press, Cambridge, England, 2020).

[5] F. J. Dyson, J. Math. Phys. (N.Y.) **3**, 140 (1962).

[6] E. P. Wigner, Ann. Math. **67**, 325 (1958).

[7] C. A. Tracy and H. Widom, Commun. Math. Phys. **159**, 151 (1994).

[8] C. A. Tracy and H. Widom, Commun. Math. Phys. **177**, 727 (1996).

[9] J. Baik, P. Deift, and K. Johansson, J. Am. Math. Soc. **12**, 1119 (1999).

[10] S. N. Majumdar and G. Schehr, J. Stat. Mech. (2014) 01012.

[11] E. P. Wigner, Math. Proc. Cambridge Philos. Soc. **47**, 790 (1951).

[12] H. A. Weidenmüller and G. E. Mitchell, Rev. Mod. Phys. **81**, 539 (2009).

[13] K. A. Takeuchi and M. Sano, Phys. Rev. Lett. **104**, 230601 (2010).

[14] M. Fridman, R. Pugatch N. Nixon, A. A. Friesem, and N. Davidson, Phys. Rev. E **85**, 020101(R) (2012).

[15] A. Lenard, J. Math. Phys. (N.Y.) **2**, 682 (1961).

[16] S. Prager, Adv. Chem. Phys. **4**, 201 (1962).

[17] R. J. Baxter, Math. Proc. Cambridge Philos. Soc. **59**, 779 (1963).

[18] A. Dhar, A. Kundu, S. N. Majumdar, S. Sabhapandit, and G. Schehr, Phys. Rev. Lett. **119**, 060601 (2017).

[19] A. Dhar, A. Kundu, S. N. Majumdar, S. Sabhapandit, and G. Schehr, J. Phys. A **51**, 295001 (2018).

[20] D. Chafaï, D. García-Zelada, and P. Jung, Bernoulli **28**, 1784 (2022).

[21] A. Flack, S. N. Majumdar, and G. Schehr, J. Stat. Mech. (2022) 053211.

[22] M. R. Evans, S. N. Majumdar, and G. Schehr, J. Phys. A **53**, 193001 (2020).

[23] A. Pal, S. Kostinski, and S. Reuveni, J. Phys. A **55**, 021001 (2022).

[24] S. Gupta and A. M. Jayannavar, Front. Phys. **10**, 789097 (2022).

[25] E. Bertin, J. Phys. A **55**, 384007 (2022).

[26] M. R. Evans and S. N. Majumdar, Phys. Rev. Lett. **106**, 160601 (2011).

[27] M. R. Evans and S. N. Majumdar, J. Phys. A **44**, 435001 (2011).

[28] M. R. Evans and S. N. Majumdar, J. Phys. A **47**, 285001 (2014).

[29] L. Kusmierz, S. N. Majumdar, S. Sabhapandit, and G. Schehr, Phys. Rev. Lett. **113**, 220602 (2014).

[30] S. N. Majumdar, S. Sabhapandit, and G. Schehr, Phys. Rev. E **91**, 052131 (2015).

[31] A. Pal, A. Kundu, and M. R. Evans, J. Phys. A **49**, 225001 (2016).

[32] S. Reuveni, Phys. Rev. Lett. **116**, 170601 (2016).

[33] M. Montero and J. Villarroel, Phys. Rev. E **94**, 032132 (2016).

[34] A. Pal and S. Reuveni, Phys. Rev. Lett. **118**, 030603 (2017).

[35] D. Boyer, M. R. Evans, and S. N. Majumdar, J. Stat. Mech. (2017) 023208.

[36] A. Chechkin and I. M. Sokolov, Phys. Rev. Lett. **121**, 050601 (2018).

[37] P. C. Bressloff, J. Phys. A **53**, 425001 (2020).

[38] R. G. Pinsky, Stoch. Proc. Appl. **130**, 2954 (2020).

[39] O. Tal-Friedman, A. Pal, A. Sekhon, S. Reuveni, and Y. Roichman, J. Phys. Chem. Lett. **11**, 7350 (2020).

[40] B. Besga, A. Bovon, A. Petrosyan, S. N. Majumdar, and S. Ciliberto, Phys. Rev. Res. **2**, 032029(R) (2020).

[41] F. Faisant, B. Besga, A. Petrosyan, S. Ciliberto, and S. N. Majumdar, J. Stat. Mech. (2021) 113203.

[42] B. De Bruyne, S. N. Majumdar, and G. Schehr, Phys. Rev. Lett. **128**, 200603 (2022).

[43] O. Vilk, M. Assaf, and B. Meerson, Phys. Rev. E **106**, 024117 (2022).

[44] E. J. Gumbel, *Statistics of Extremes* (Dover, New York, 1958).

[45] H. A. David and H. N. Nagaraja, *Order Statistics* (John Wiley & Sons, New York, 2004).

[46] G. Schehr and S. N. Majumdar, in *First-Passage Phenomena and Their Applications*, edited by R. Metzler, G. Oshanin, and S. Redner (World Scientific, Singapore, 2014), pp. 226–251.

[47] S. N. Majumdar, A. Pal, and G. Schehr, Phys. Rep. **840**, 1 (2020).

[48] See Supplemental Material at http://link.aps.org/supplemental/10.1103/PhysRevLett.130.207101 for detailed computations which includes Refs. [49-53].

[49] M. M. Fogler and B. I. Shklovskii, Phys. Rev. Lett. **74**, 3312 (1995).

[50] O. Costin and J. L. Lebowitz, Phys. Rev. Lett. **75**, 69 (1995).

[51] S. N. Majumdar, C. Nadal, A. Scardicchio, and P. Vivo, Phys. Rev. Lett. **103**, 220603 (2009).

[52] R. Marino, S. N. Majumdar, G. Schehr, and P. Vivo, Phys. Rev. Lett. **112**, 254101 (2014).

[53] N. R. Smith, P. Le Doussal, S. N. Majumdar, and G. Schehr, SciPost Phys. **11**, 110 (2021).

[54] J. Gustavsson, Ann. Inst. Henri Poincaré-Pr. **41**, 151 (2005).

[55] I. A. Martinez, A. Petrosyan, D. Guéry-Odelin, E. Trizac, and S. Ciliberto, Nat. Phys. **12**, 843 (2016).